

Photoionization mass spectrometric study of Si_2H_6

B. Ruscic and J. Berkowitz

Chemistry Division, Argonne National Laboratory, Argonne, Illinois 60439

(Received 13 February 1991; accepted 9 May 1991)

The adiabatic I.P. of Si_2H_6 obtained by a photoionization mass spectrometric study at two temperatures is 9.74 ± 0.02 eV. The first fragment, Si_2H_4^+ , initially appears with a shallow slope at $<10.04 \pm 0.02$ eV, and with a much steeper slope at $<10.81 \pm 0.02$ eV. It is argued that the initial onset corresponds to formation of $\text{H}_2\text{SiSiH}_2^+$, while the steeper onset is attributed to formation of H_3SiSiH^+ . The second fragment, Si_2H_5 , has an appearance potential of $<11.59 \pm 0.02$ eV (11.41 ± 0.03 is a probable value). Successive decomposition leads to Si_2H_2^+ (from Si_2H_4^+) and Si_2H_3^+ (from Si_2H_5^+). The photoion yield curve for Si_2H_3^+ also displays shallow and steep onsets. Upper limits for the appearance potentials can be readily extracted, but the true thermochemical onsets are less well defined. Heats of formation (or upper limits) are presented for each of these species. For Si_2H_6^+ , Si_2H_5^+ , and Si_2H_4^+ , the experimental values are in good agreement with recent *ab initio* calculations. For the daughter species, the experimental values exceed the calculated ones, as expected.

I. INTRODUCTION

The motivation for experimental studies of simple silicon hydride species has both a technological and a fundamental aspect. The technological aspect involves the production of thin films of silicon by chemical vapor decomposition in the microelectronics industry. Mandich, Reents, and Kolenbrander¹ have recently studied the rates of ion—molecule clustering reactions, testing them as possible precursors of condensation nuclei. Other mechanisms involve neutral free radicals. As they point out, considerable experimental and theoretical work has been directed over the past two decades towards understanding the gas-phase chemistry of silanes. A prerequisite for sorting through the many possible reactions is the availability of accurate thermochemical data. Recently, both experimental² and *ab initio* calculational³ approaches have converged on the values for the heats of formation of SiH_n and SiH_n^+ ($n = 1-4$) species. For the Si_2H_n and Si_2H_n^+ ($n = 1-6$) species (except for Si_2H_6), the major information to date is calculational.⁴⁻²² The species Si_2H_n ($n = 1-5$) have not yet been prepared and isolated for study. The experimental information on Si_2H_n^+ is based on electron-impact and ion-impact studies, whose accuracy could perhaps be improved.

The fundamental aspect concerns the different bonding in silicon and carbon hydrides. *Ab initio* calculations^{7,8,10,11,16} indicate that the stable form of Si_2H_2 is cyclic—the triply bonded form may not even be a local minimum on the potential surface. Although studies of germanium compounds are not as extensive, a recent *ab initio* calculation²³ predicts that the lowest-lying structure of Ge_2H_2 is also C_{2v} dibridged, "... surprisingly similar" to Si_2H_2 . Hence, at this early stage of our understanding, it appears as if major changes in chemical and structural behavior occur between C_2H_n and Si_2H_n , but that relatively minor changes may ensue for heavier members of the series (although metallic behavior for Sn and Pb probably involves further changes).

Another remarkable result of *ab initio* calculations is that the stable form of Si_2H_3^+ is predicted^{4,15} to be triply bridged (D_{3h} symmetry), quite different from that of vinyl cation. Multiple bonding is generally believed to be much weaker in Si—Si compounds than in C—C compounds. This view could be quantified if accurate heats of formation were available.

Our goal in the present study was to obtain more precise values of ionization and appearance potentials from Si_2H_6 , by photoionization mass spectrometry.

In the following paper,²⁴ we describe a method used to prepare the transient species Si_2H_5 , Si_2H_4 , Si_2H_3 , and Si_2H_2 . Ionization potentials are obtained, which are then combined with appropriate appearance potentials to deduce the heats of formation of these transient species, or equivalently, the successive Si—H bond energies.

II. EXPERIMENTAL ARRANGEMENT

The basic photoionization mass spectrometric apparatus, involving a gaseous discharge light source, a 3 m vacuum-ultraviolet monochromator, and a quadrupole mass spectrometer has been described previously.^{2,25} The nominal wavelength resolution was 0.84 \AA . In addition to room-temperature experiments, some measurements were performed with the disilane gas cooled to $t \approx -105 \text{ }^\circ\text{C}$ prior to photoionization.

Disilane was obtained from Matheson Gas Products and used without further purification.

III. EXPERIMENTAL RESULTS

A. Overview of the photoionization mass spectrum

Figure 1(a) is a reproduction of the He I photoelectron spectrum of Si_2H_6 .²⁶ Figure 1(b) [same energy scale as Fig. 1(a)] displays the photoion yield curves of the major disilicon ionic species resulting from photoionization of Si_2H_6 . In the construction of Fig. 1(b), it was necessary to take into account the isotopic abundances of the silicon isotopes²⁷

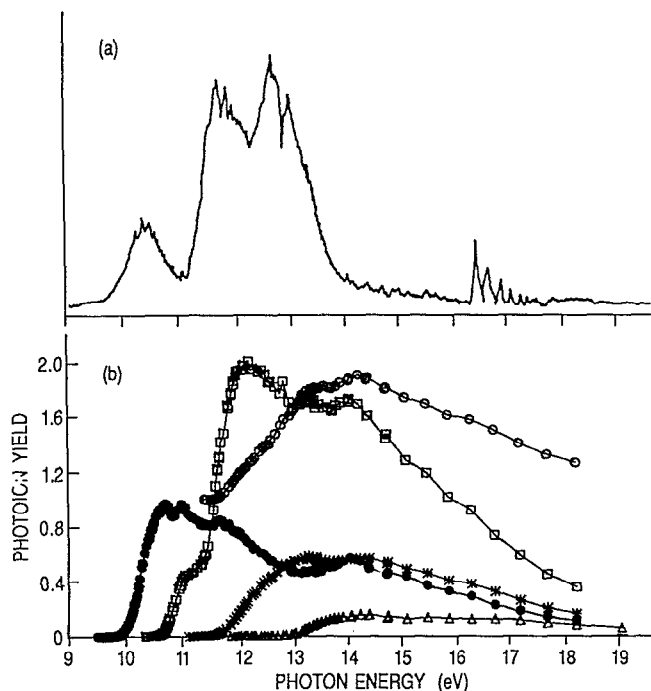


FIG. 1. (a) He I photoelectron spectrum of Si_2H_6 . (From Ref. 26, with permission of the author). (b) Photoion yield curves of major Si_2H_n^+ species from Si_2H_6 . \bullet , Si_2H_6^+ ; \square , Si_2H_4^+ ; $*$, Si_2H_3^+ ; \triangle , Si_2H_2^+ ; \circ , Si_2H^+ , with zero offset to 1.0 for clarity.

($^{28}\text{Si} = 92.23\%$; $^{29}\text{Si} = 4.67\%$; $^{30}\text{Si} = 3.10\%$). For example, Si_2H_4^+ rapidly becomes the strongest ionic species. Its largest component occurs at M60, $^{28}\text{Si}^{28}\text{SiH}_4^+$. The contribution of $^{29}\text{Si}^{28}\text{SiH}_4^+$ is significant, especially near threshold, at M61, and must be taken into account in evaluating the photoion yield of $^{28}\text{Si}^{28}\text{SiH}_5^+$. This correction had apparently not been made in an earlier electron-impact study.²⁸ In addition, due to incomplete mass separation, a small quantity ($\sim 0.3\%$) of leakage occurred from a given mass M to $M - 1$, and this was also taken into account. Mass discrimination due to the transmission properties of the quadrupole mass spectrometer was concluded to be slight for the disilicon species [by comparing the intensities of M62 ($^{28}\text{Si}^{28}\text{SiH}_6^+$) and M64 ($^{30}\text{Si}^{28}\text{SiH}_6^+ + ^{29}\text{Si}^{29}\text{SiH}_6^+$) with the known isotopic abundances]. However, when comparing SiH_n^+ with Si_2H_n^+ (see below) the discrimination factor is probably significant. The intensities in Fig. 1 (b) should be equivalent to those which would be obtained using monoisotopic Si_2H_6 .

Much lower intensities are observed for Si_2H^+ and Si_2^+ , the latter only detectable when plotting the ratio of M56 (Si_2^+) to that of M58 (Si_2H_2^+), as shown in Fig. 2(a). In Fig. 2(b), the SiH_3^+ and SiH_2^+ photoion yield curves are displayed. The curve for SiH_2^+ is not significant, since several criteria can be used to show that some SiH_4 exists in the sample, e.g., the ratio of $\text{SiH}_n^+ : \text{Si}_2\text{H}_n^+$ differs from run to run, as does the relative abundance of SiH_3^+ to SiH_2^+ . Also, the appearance energy of SiH_2^+ is about the same as it is from

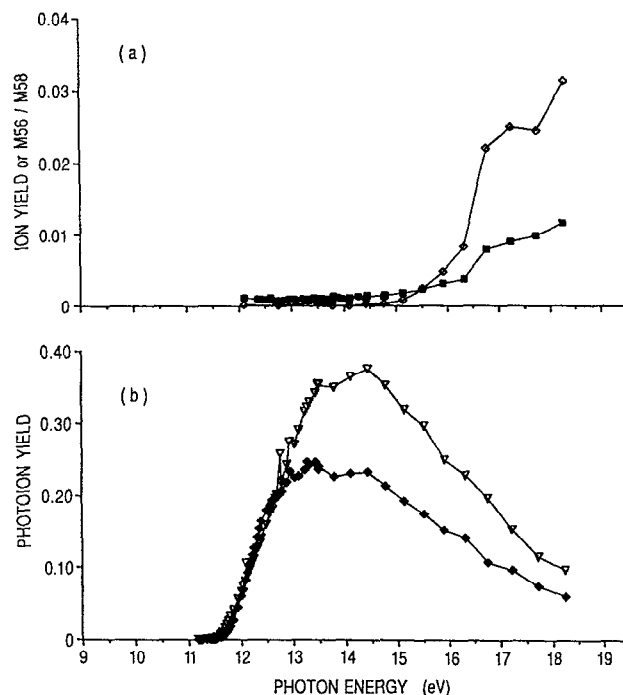


FIG. 2. (a) Photoion yield curve of Si_2H^+ from Si_2H_6 (\diamond) and the ratio of Si_2^+ to Si_2H_2^+ , as measured by the M56 to M58 intensity ratio (\blacksquare). (b) Photoion yield curves of SiH_3^+ (∇) and SiH_2^+ (\blacklozenge) from Si_2H_6 . The SiH_2^+ curve is contaminated by formation of SiH_2^+ from some SiH_4 impurity.

SiH_4 . However, the appearance energy of SiH_3^+ (~ 11.6 eV) is lower than from SiH_4 , and hence it must derive (near threshold) from Si_2H_6 .

B. Ionization and appearance potentials from Si_2H_6

1. Si_2H_6^+ (Si_2H_6)

The photoion yield curve of Si_2H_6^+ (Si_2H_6) in the threshold region is given in Fig. 3. (The Si_2H_6^+ ion intensity

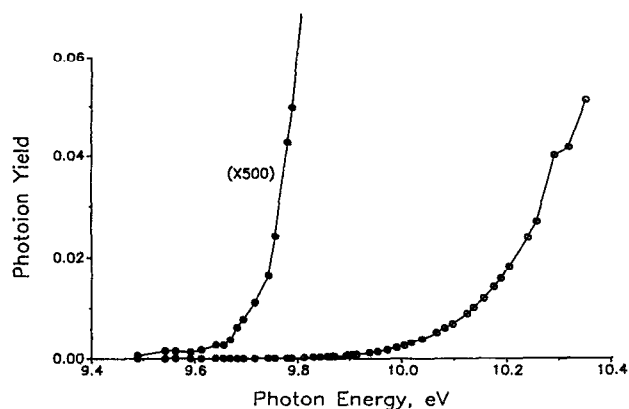


FIG. 3. The photoion yield curve of Si_2H_6^+ (Si_2H_6) in the threshold region obtained at room temperature.

is monitored at M62; isotopic contamination is negligible near threshold.) Both the photoelectron spectrum [Fig. 1(a)] and the Si₂H₆⁺ photoion yield curve exhibit a gradual approach to threshold. In principle, such a slowly increasing curve could be due to a broad Franck–Condon distribution, or to “hot bands”—ionization from vibrationally excited states of Si₂H₆ populated at room temperature. Watanabe²⁹ introduced the tactic of plotting the photoion yield curve near threshold on semilogarithmic coordinates. In such a display, ionization from Boltzmann excited states appears as a linear function below the adiabatic threshold. Departure from linearity signals the onset of the true adiabatic ionization potential. One problem with this approach is that declining Franck–Condon factors may also appear as a linear function on semilogarithmic coordinates.

In an attempt to distinguish between these effects, we performed a photoionization study of cooled Si₂H₆ (*t* = −105 ± 10 °C) in the threshold region. The resulting photoion yield curve is shown in Fig. 4. It is difficult to see any significant difference in threshold, or indeed to select a threshold on this scale. When both data sets are magnified (×500), one can begin to see a small shoulder to lower energy in the room-temperature experiment (Fig. 3). Hence, we conclude that the tailing toward threshold is primarily due to weak Franck–Condon factors, rather than Boltzmann effects. Our inferred adiabatic onset (9.74 ± 0.02 eV) is listed in Table I, and compared with electron-impact values [10.15 ± 0.10 eV (Ref. 28); 9.9 ± 0.4 eV (Ref. 30)], thresholds inferred from the photoelectron spectrum [10.0 (Ref. 31) and 9.7 eV (Ref. 32)], and a recently calculated value, 9.70 eV.²²

2. Si₂H₄⁺ (Si₂H₆)

The photoion yield curve of Si₂H₄⁺ (Si₂H₆) in the threshold region, monitored on M60, is shown in two stages of amplification in Fig. 5(a). At an amplification of approximately a factor 5 compared to Fig. 1(b), one observes a linear segment with what appears to be an asymptotic tailing toward the background level. The extrapolation of the linear region to the base line yields a threshold of 10.71 ± 0.02 eV.

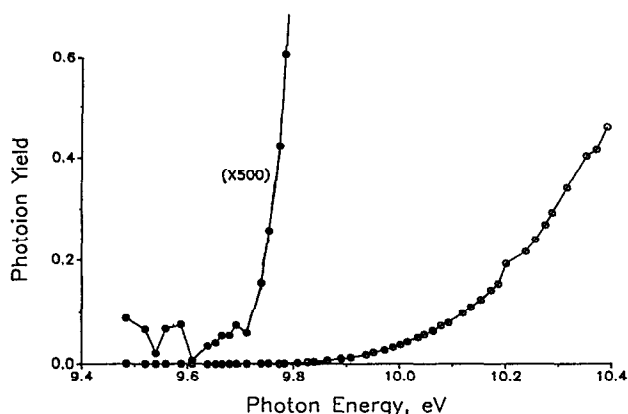


FIG. 4. The photoion yield curve of Si₂H₆⁺ (Si₂H₆) in the threshold region, obtained at *t* = −105 ± 10 °C.

With an internal energy correction³³ for Si₂H₆ at 300 K of 0.101 eV, one obtains a 0 K onset of 10.81 ± 0.02 eV. This value appears to be in good agreement with prior electron-impact appearance potentials of 10.85 ± 0.10 eV (Ref. 28) and 10.8 ± 0.4 eV.³⁰

However, with a further amplification of a factor 40 [Fig. 5(a)], the asymptotic tailing now appears as a weak, quasilinear region with a much shallower slope, merging into the strong ionization process which has a steep slope. The shallow slope approaches the background level at 9.94 ± 0.02 eV (10.04 eV at 0 K). We shall present the case (see below) that the lower (and weaker) appearance potential corresponds to formation of symmetric H₂Si–SiH₂⁺, and the higher, more intense onset signals the formation of the asymmetric H₃Si–SiH⁺.

In Fig. 5(b), we introduce a different display of the data. If step-function photoionization behavior prevails, then it can be shown³⁴ that the derivative of the photoion yield curve of a fragment should have a shape similar to a photoelectron–photoion coincidence curve of that fragment. The curve in Fig. 5(b) is such a derivative, obtained from a spline function fitted to the photoion yield curve of Si₂H₄⁺ near threshold. As expected, this derivative curve reaches the base line at a significantly higher energy than that corresponding to the weak process. The apparent threshold is ~10.6 eV, rather than the 10.71 eV obtained from linear extrapolation of the strong process. This difference reflects the curvature near the onset, as the weak process merges into the strong one.

3. Si₂H₅⁺ (Si₂H₆)

The photoion yield curve of Si₂H₅⁺ (Si₂H₆) in the threshold region, shown in Fig. 6, has pronounced curvature as it approaches the base line. If one nevertheless attempts a linear extrapolation, intersection with the base line occurs at ~11.73 eV. However, if we amplify the region near threshold (×50), a linear portion is evident, which extrapolates to 11.49 ± 0.02 eV. In the analogous decomposition C₂H₆⁺ → C₂H₅⁺, the onset is ambiguous because of curvature near threshold, and also because of a weak, interfering ion-pair process (C₂H₅⁺ + H[−]). In both the disilane and ethane cases, there is a fragment of lower energy (Si₂H₄⁺, C₂H₄⁺) which will be formed by rapid unimolecular decay at the threshold for H-atom loss. Before the H-atom loss process can compete successfully, some excess energy must be imparted to the parent Si₂H₆⁺, resulting in a delayed threshold, or “kinetic shift.” However, the first appearance of C₂H₅⁺ in a coincidence experiment³⁵ occurs (within experimental error) at the thermochemical onset. (The heat of formation of C₂H₅⁺ has been established by examining the appearance potential of this ion from several ethyl halides.³⁶) This may be due to the fortuitous cancellation of an internal thermal energy shift to lower energy, and a kinetic shift to higher energy.

In Fig. 7, we display the derivative of the photoion yield curve, which is expected to simulate a coincidence curve (see above). It approaches the base line at 11.41 ± 0.03 eV. If we assume that a similar cancellation of thermal shift and kinet-

TABLE I. Ionization and appearance potentials of species produced by ionization of Si_2H_6 (in eV). In the present results, the quantities without parentheses are rigorous upper limits, quantities in parentheses are probable lower values. PES denotes photoelectron spectroscopy.

	Present results (0 K)	Potzinger and Lampe ^a	Potzinger <i>et al.</i> ^b	Steele and Stone ^c	Chatham <i>et al.</i> ^d	Curtiss <i>et al.</i> ^e
Si_2H_6^+	9.74 ± 0.02	10.15 ± 0.10	10.0 (PES)	...	9.9 ± 0.4	9.70
Si_2H_5^+	$<11.59 \pm 0.02$ (11.41 ± 0.03)	11.40 ± 0.10	11.4	...	11.2 ± 0.4	11.45
Si_2H_4	$<10.04 \pm 0.02$ (sym) $<10.81 \pm 0.02$ (asym)	10.85 ± 0.10	10.8 ± 0.4	10.09 (sym) 10.68 (asym)
Si_2H_3^+	$<13.00 \pm 0.04$ (<12.70)	12.50 ± 0.10	12.0 ± 1	12.54
Si_2H_2^+	$<11.72^{+0.02}_{-0.04}$ ($<11.57 \pm 0.03$)	11.80 ± 0.10	11.5	11.36
Si_2H^+	<15.0	12.90 ± 0.2	15 ± 2	14.53
Si_2^+	<14.5	13.0	17.5 ± 3	13.13
SiH_3^+	$<11.72 \pm 0.02$	11.95 ± 0.15	11.75	11.85 ± 0.05	11.0 ± 2	...
SiH_2^+	...	11.95 ± 0.10	11.95	11.94 ± 0.04	10.0 ± 2	...
SiH^+	14.0 ± 2
...
Si^+	15 ± 2
...

^a Reference 28.

^b Reference 31.

^c W. C. Steele and F. G. A. Stone, *J. Am. Chem. Soc.* **84**, 3599 (1962).

^d Reference 30.

^e Reference 22.

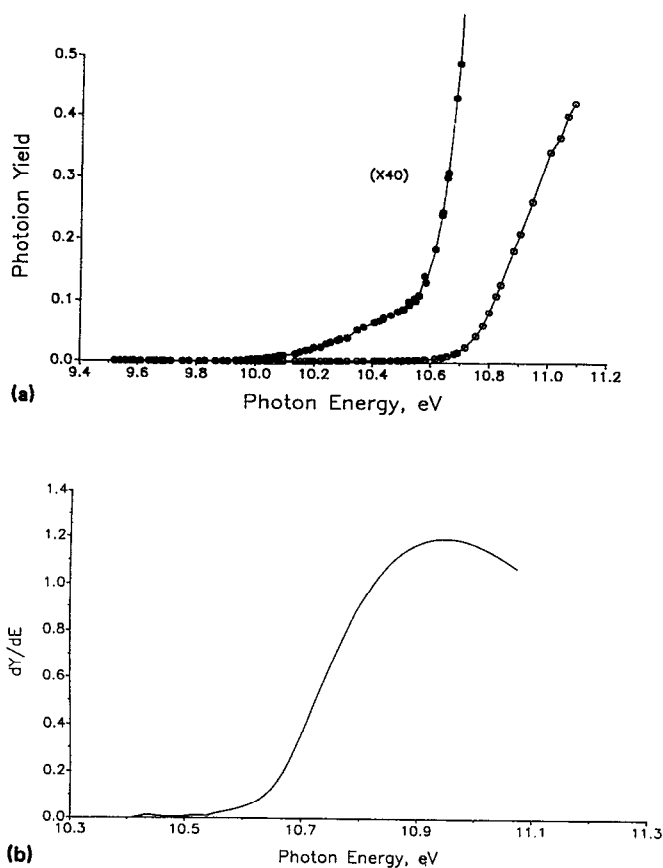


FIG. 5. (a) The photoion yield curve of Si_2H_4^+ (Si_2H_6) in the threshold region. (b) Derivative of the photoion yield curve of (a), after smoothing.

ic shift occurs here, then this would be the thermochemical appearance potential. More rigorously, the *upper limit* to this threshold is obtained from the extrapolated, amplified curve in Fig. 6, which yields a 0 K onset of 11.59 ± 0.02 eV.

4. Si_2H_3^+ (Si_2H_6)

From Fig. 1(b), it is apparent that both Si_2H_4^+ (M60) and Si_2H_2^+ (M58) have lower energy thresholds than does Si_2H_3^+ (M59). Hence, both M60 and M58 have substantial

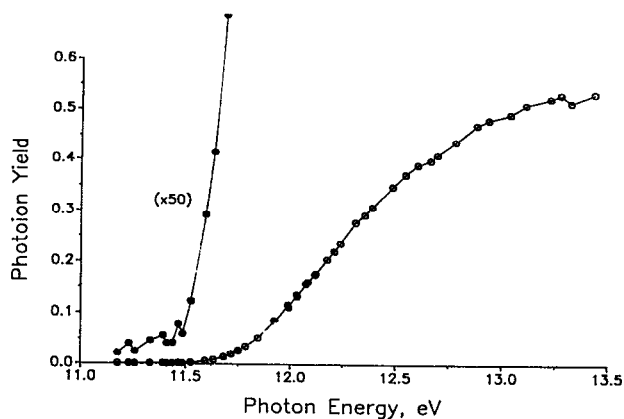


FIG. 6. The photoion yield curve of Si_2H_3^+ (Si_2H_6) in the threshold region.

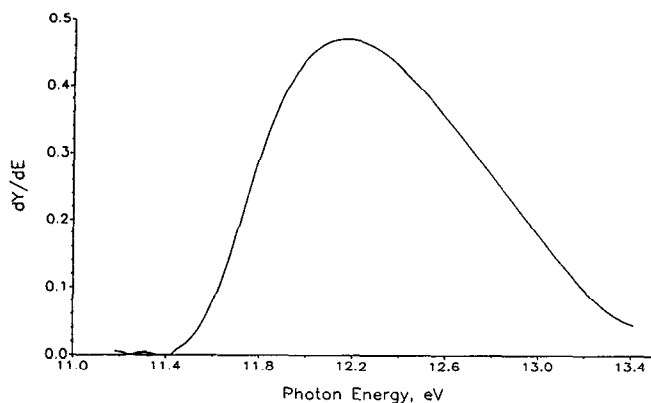


FIG. 7. Derivative of the photoion yield curve of Fig. 6, after smoothing.

ion intensities in the vicinity of the threshold of M59, and corrections (mass leakage, isotopic) must be made to the M59 ion intensity in order to extract that component which can be identified with Si_2H_3^+ . This has been done for the data in Fig. 1(b), and also the threshold region shown in Fig. 8. There are two problems in interpreting this threshold, in addition to that discussed for Si_2H_5^+ (see above).

(a) The decomposition process leading to Si_2H_3^+ is almost certainly $\text{Si}_2\text{H}_6^+ \rightarrow \text{Si}_2\text{H}_5^+ \rightarrow \text{Si}_2\text{H}_3^+$. Since this is a consecutive reaction, it could lead to a larger kinetic shift.

(b) Elsewhere,²⁴ we show that decomposition of Si_2H_5^+ occurs more readily to a structure SiSiH_3^+ or a single-hydrogen bridged structure than it does to the ground-state structure, $\text{Si}(\text{H}_3)\text{Si}^+$. As a consequence, the clear (strong) threshold observed very likely reflects the formation of SiSiH_3^+ or $\text{HSi}(\text{H})\text{SiH}^+$, which lie about 0.5 eV above the ground-state structure.

As one measure of the effect described in (a), we make reference to the analogous decomposition of C_2H_6^+ to C_2H_3^+ measured by coincidence spectroscopy.³⁵ In this experiment, the measured onset of C_2H_3^+ occurs at the thermochemical onset (14.53 eV), within a small experimental un-

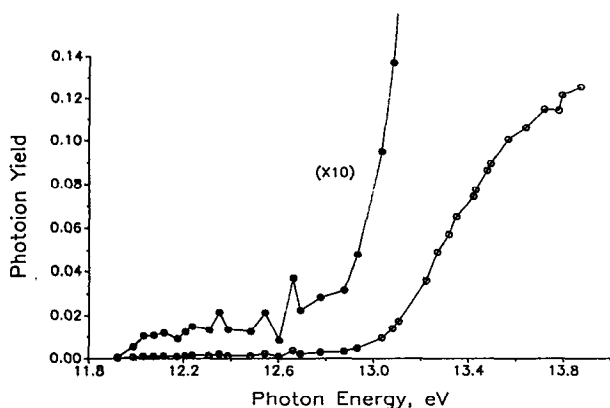


FIG. 8. The photoion yield curve of Si_2H_3^+ (Si_2H_6) in the threshold region.

certainty. Hence, the thermal and kinetic shifts approximately cancel once again.

In Fig. 8, one can see the onset of a strong process at 12.90 ± 0.04 eV (13.00 ± 0.04 eV at 0 K), with some tailing. In the amplified ($\times 10$) curve, the first significant point above the background level occurs at 12.66 eV; the next lower point is at 12.60 eV. If this corresponds to a weak threshold, its onset occurs in this interval. The *ab initio* calculations imply that there should be an onset for $\text{Si}(\text{H}_3)\text{Si}^+$ roughly 0.5 eV below the strong threshold, but the probability of its formation may be very small.

In summary, the appearance potential of Si_2H_3^+ (Si_2H_6) is rigorously $\leq 13.00 \pm 0.04$ eV at 0 K. There may be some experimental evidence for a weak threshold at ~ 12.60 eV (12.70 eV at 0 K), which is about 0.2 eV higher than that expected from *ab initio* calculations. The appearance potential of Si_2H_3^+ (Si_2H_6) given by Potzinger and Lampe²⁸ is in fact 12.50 ± 0.10 eV, but it is probably artificially low, because of isotopic contamination from ^{29}Si $^{28}\text{SiH}_2^+$. These and other values for Si_2H_3^+ are given in Table I.

5. Si_2H_2^+ (Si_2H_6)

This species, monitored at M58, has no significant corrections. Isotopic contamination from M57 (Si_2H^+) and leakage from M59 (Si_2H_3^+) cannot occur near the threshold region of Si_2H_2^+ , since those other species have higher appearance potentials [cf. Fig. 1(b)]. Although M60 (Si_2H_4^+) is intense in this region, the leakage two masses lower has been measured to be $\sim 10^{-4}$ of the peak intensity. The photoion yield curve of Si_2H_2^+ (Si_2H_6) in the threshold region is shown in Fig. 9. The problems with interpretation of this threshold are similar to those encountered for Si_2H_3^+ (Si_2H_6). Si_2H_2^+ results from the consecutive processes $\text{Si}_2\text{H}_6^+ \rightarrow \text{Si}_2\text{H}_4^+ \rightarrow \text{Si}_2\text{H}_2^+$. Hence one can anticipate a substantial kinetic shift. For the analogous decomposition of C_2H_6^+ , the onset observed³⁵ in a coincidence experiment (~ 14.75 eV) is significantly higher than the thermochemical onset (14.47 eV). In addition, the ground-state structure^{21,22,24} of Si_2H_2^+ is cyclic $\text{Si}(\text{H}_2)\text{Si}^+$. A barrier is believed to exist²¹ in the final decomposition stage ($\text{Si}_2\text{H}_4^+ \rightarrow \text{Si}_2\text{H}_2^+ + \text{H}_2$). Hence, on two counts the threshold observed is likely to be well above the thermochemical threshold.

From the amplified ($\times 50$) threshold photoion yield curve shown in Fig. 9, we obtain an extrapolated onset at 11.62 ± 0.02 eV, or 11.72 ± 0.04 eV at 0 K. The derivative of the Si_2H_2^+ photoion yield curve is displayed in Fig. 10. From this curve, we infer a threshold of 11.57 ± 0.03 eV. If the analogy with C_2H_2^+ (C_2H_6) is appropriate, even this latter value may be ~ 0.3 eV too high. An analysis based on additional data is given elsewhere.²⁴ It is noteworthy that Potzinger and Lampe²⁸ give 11.80 ± 0.10 eV for this appearance potential. Electron-impact appearance potentials are usually higher than those obtained by photoionization, and hence the discrepancy here can be considered normal. It reinforces our view that the appearance potentials of Si_2H_5^+ and Si_2H_3^+ were lowered in the electron-impact experi-

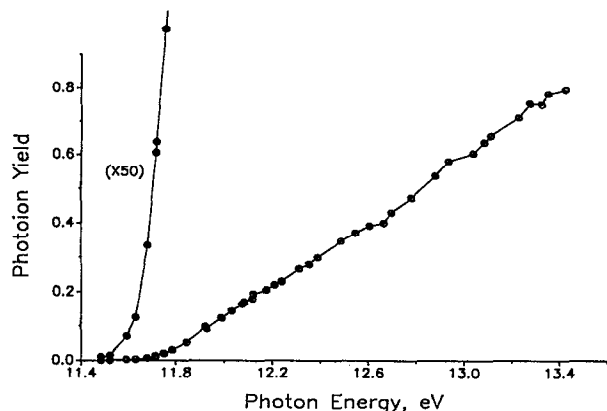


FIG. 9. The photoion yield curve of Si_2H_2^+ (Si_2H_6) in the threshold region.

ments by isotopic contamination, which is not present for Si_2H_2^+ . Table I summarizes those and other results for appearance potentials (Si_2H_2^+).

6. Si_2H^+ and Si_2^+ from Si_2H_6

These are weak fragments, presumably formed in a longer chain of successive decompositions (i.e., $\text{Si}_2\text{H}_6^+ \rightarrow \text{Si}_2\text{H}_4^+ \rightarrow \text{Si}_2\text{H}_2^+ \rightarrow \text{Si}_2^+$). The observed threshold for Si_2H^+ [< 15.0 eV from Fig. 2(a)] is not expected to have thermochemical significance, except as a crude upper limit. The Si_2^+ ion intensity is an order of magnitude weaker than that of Si_2H^+ . Indeed, the background at M56 (Si_2^+) makes the extraction of any signal difficult. It appears to be due to decomposition of Si_2H_2^+ by collisions. Hence, a plot of the ratio of intensities of M56 and M58 appears to be the most reliable way of establishing any significant signal attributable to Si_2^+ (Si_2H_6). From Fig. 2(a), the onset of Si_2^+ is < 14.5 eV.

7. SiH_3^+ and SiH_2^+

As mentioned earlier, the significance of the SiH_2^+ photoion yield curve is dubious, since evidence exists that the

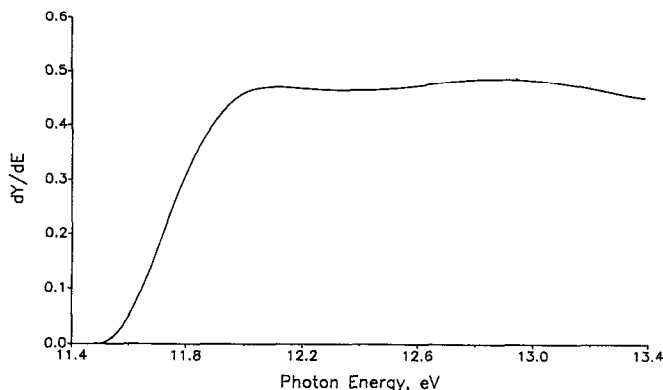


FIG. 10. Derivative of the photoion yield curve of Fig. 9, after smoothing.

Si_2H_6 sample slowly decomposes while in the vacuum line, and the monosilicon hydride ions can result from photoionization of SiH_4 . This is particularly true for SiH_2^+ , which appears to have almost the same onset here as found previously² for SiH_2^+ (SiH_4). However, the SiH_3^+ photoion yield curve [Fig. 2(b)] has a rather long linear segment, unlike the corresponding threshold portion of SiH_3^+ (SiH_4)², which had pronounced curvature in its approach to threshold. In addition, the extrapolated linear segment of Fig. 2(b) reaches the background level at 11.62 ± 0.02 eV ($< 11.72 \pm 0.02$ eV at 0 K), well below the limit² (< 12.086 eV) established for SiH_3^+ (SiH_4). Hence, the threshold obtained from Fig. 2(b) can be reliably attributed to SiH_3^+ (Si_2H_6).

The appearance potentials of all of the species derived from Si_2H_6 are summarized on Table I, and compared with earlier values in the literature, and with a recent calculation. The experimental electron-impact values of Chatham, *et al.*³⁰ have a large uncertainty, and (surprisingly) are significantly lower than the photoionization values in several cases. The measured values of Potzinger and Lampe²⁸ are closer to the photoionization values. They are lower, especially for Si_2H_3^+ , where isotopic contamination is significant. The *ab initio* calculated values of Curtiss *et al.*²² are in reasonably good agreement with the photoionization values for Si_2H_6^+ , Si_2H_5^+ , and Si_2H_4^+ . For the lower fragments, the calculated values are lower, as expected, due to delayed onsets in the photoionization measurements discussed in the preceding text.

IV. INTERPRETATION OF RESULTS

A. The $\text{Si}_2\text{H}_6 \rightarrow \text{Si}_2\text{H}_6^+$ transition

We had concluded in Sec. III B. that the gradual onset of Si_2H_6^+ (Si_2H_6) was primarily attributable to a broad Franck-Condon distribution, rather than thermal (Boltzmann distribution) effects. The first band in the photoelectron spectrum [Fig. 1(a)] has a width of ~ 1 eV, which also implies a broad Franck-Condon distribution. However, it also has some partially resolved vibrational structure, with a spacing of ~ 0.11 eV ≈ 900 cm^{-1} . According to Franck-Condon analysis, the active frequencies should be totally symmetric, and should reflect the change in structure between the ground states of Si_2H_6 and Si_2H_6^+ .

According to recent calculations by Curtiss *et al.*,²² both structures have D_{3d} symmetry. The detailed structure calculated for Si_2H_6 ($r_{\text{SiH}} = 1.487$ Å, $r_{\text{SiSi}} = 2.335$ Å, $\angle \text{SiSiH} = 110.4^\circ$) is very close to the experimental structure.³⁷ Hence, since the calculations for the cation and neutral were performed at the same level, we assume that the calculated cation structure is of comparable accuracy. The detailed structure calculated for Si_2H_6^+ is $r_{\text{SiH}} = 1.471$ Å, $r_{\text{SiSi}} = 2.659$ Å, $\angle \text{SiSiH} = 98.3^\circ$. The major structural changes upon ionization involve a drastic increase (0.324 Å) in the Si-Si distance, and a significant change in the H_3Si pyramidal angle.

There are three totally symmetric normal modes in Si₂H₆ (and Si₂H₆⁺). One involves symmetric Si–H stretching, and is calculated to occur at ~2460 cm⁻¹ (~2215 cm⁻¹ when reduced by 10%, as comparison with experiment³⁸ suggests). The other two involve in-phase SiH₃ umbrella motion (calculated $\omega = 918.7$ cm⁻¹; reduced $\omega = 827$ cm⁻¹) and the Si–Si stretch (calculated $\omega = 242.5$ cm⁻¹; reduced $\omega = 221$ cm⁻¹). Since the major structural changes involve the Si–Si distance and the H₃Si pyramidal angle, we anticipate that the Franck–Condon active modes will be the ones with $\omega \sim 900$ cm⁻¹ and $\omega \sim 230$ cm⁻¹. The latter is probably too small to be resolved in the photoelectron spectrum, although there are some wiggles which appear outside of statistical uncertainty. It seems likely that the breadth of the first photoelectron band, and the gradual approach to threshold, primarily involve this low-frequency mode correlated with the large change in Si–Si distance. The partially resolved fine structure atop the first band is then attributed to a Franck–Condon progression in the SiH₃ umbrella mode.

B. Heats of formation of cations: structural implications

1. Si₂H₄⁺ and Si₂H₆⁺

In Sec. III B 2, we described two thresholds for Si₂H₄⁺ from Si₂H₆—a weak threshold at 10.04 eV, and a strong one at <10.81 eV. We attributed the low threshold to formation of the symmetric H₂Si–SiH₂⁺, and the higher threshold to the asymmetric H₃Si–SiH⁺. This assignment is supported by the recent *ab initio* calculations of Curtiss *et al.*,²² who obtain an energy threshold of 10.09 eV for the symmetric Si₂H₄ from Si₂H₆, and 10.68 eV for the asymmetric Si₂H₄⁺.

The loss of H₂ from neutral Si₂H₆ has been examined by *ab initio* calculations,^{9,14} and a similar behavior is observed. A large reverse activation barrier (40–50 kcal/mol) is found for decomposition to symmetric Si₂H₄, but at most a very small reverse activation barrier for decomposition to the asymmetric Si₂H₄, although the symmetric form is calculated to be more stable. Raghavachari³⁹ has calculated a reverse activation barrier of 20 kcal/mol for decomposition of Si₂H₆⁺ into symmetric Si₂H₄⁺ + H₂. Such a large barrier is difficult to rationalize with our inference of a measured threshold for symmetric Si₂H₄⁺, albeit weak. That a barrier exists is not surprising. The symmetric H₂Si–SiH₂⁺ is difficult to form from Si₂H₆⁺ because it implies a tight, four-center transition state. From the calculated structure²² of Si₂H₆⁺, the H...H distance (H's from different Si atoms) is 3.08 Å. Hence, a substantial distortion is required to form the transition state. Formation of the asymmetric H₃Si–SiH⁺ involves a three-center transition state, which is less constrained and similar to the corresponding process in C₂H₆⁺. A similar situation was encountered in earlier work in this laboratory on the decomposition of H₂NOH⁺.⁴⁰ The lower-energy fragment, HNO⁺, involves H₂ loss by H atoms from opposite ends of the molecule, whereas NOH⁺ is formed when the H atoms on the nitrogen end join to form H₂. Both processes are observed, but the lower-energy pro-

cess is weaker. In the decomposition process C₂H₆⁺ → C₂H₄⁺ + H₂, the primary contribution to C₂H₄⁺ is the symmetric ethylene-like structure. In the following paper,²⁴ we show that the C–C bond in C₂H₄⁺ is significantly stronger than the Si–Si bond in H₂Si–SiH₂⁺. In addition, the distance between H atoms on opposite carbons is not as large. However, even in this case the formation of H₃C–CH⁺ is not insignificant. Prasil and Forst,⁴¹ who calculated the breakdown diagram for C₂H₆⁺, noted that "...without postulating the existence of the structure CH₃CH⁺ it would have been quite impossible to fit the observed abundance of C₂H₂⁺."

In order to arrive at heats of formation of the cations measured in this experiment, it is necessary to know $\Delta H_f^0(\text{Si}_2\text{H}_6)$. The experimental value of Gunn and Green⁴² is $\Delta H_{f,298}^0(\text{Si}_2\text{H}_6) = 17.1 \pm 0.3$ kcal/mol. Most compilers and researchers in recent years have added 2 kcal/mol to this quantity, arguing that the product silicon formed in the calorimetric experiment was amorphous, with a heat of formation 1 kcal/mol higher than crystalline silicon (the standard state). For consistency, we make the same assumption here. From the experimental frequencies of Si₂H₆,³⁸ we calculate $\Delta H_{f,0}^0(\text{Si}_2\text{H}_6) = 22.9 \pm 0.3$ kcal/mol. Consequently, $\Delta H_{f,0}^0(\text{Si}_2\text{H}_6^+) = 247.5 \pm 0.6$ kcal/mol, $\Delta H_{f,0}^0(\text{Si}_2\text{H}_4^+, \text{sym}) = 254.4 \pm 0.6$ kcal/mol, and $\Delta H_{f,0}^0(\text{Si}_2\text{H}_4^+, \text{asym}) \leq 272.2 \pm 0.6$ kcal/mol.

2. Si₂H₅⁺

From the analysis given in Sec. III B 3, we obtain as an upper limit $\Delta H_{f,0}^0(\text{Si}_2\text{H}_5^+) \leq 238.5 \pm 0.6$ kcal/mol, utilizing the well-established⁴³ $\Delta H_{f,0}^0(\text{H})$. The probable value is $\Delta H_{f,0}^0(\text{Si}_2\text{H}_5^+) = 234.4 \pm 0.8$ kcal/mol.

3. Si₂H₃⁺

A rigorous upper limit is $\Delta H_{f,0}^0(\text{Si}_2\text{H}_3^+) \leq 271.1 \pm 0.9$ kcal/mol. A possible lower value, based on a very weak and ill-defined threshold, is <264 kcal/mol. This value could correspond to formation of a different Si₂H₃⁺ structure.

4. Si₂H₂⁺

A rigorous upper limit is $\Delta H_{f,0}^0(\text{Si}_2\text{H}_2^+) \leq 293.1 \pm 0.6$ kcal/mol. A less-rigorous, but probable upper limit is $\Delta H_{f,0}^0(\text{Si}_2\text{H}_2^+) \leq 289.7 \pm 0.8$ kcal/mol. The true thermochemical value may be 6–7 kcal/mol lower.

5. Si₂H⁺ and Si₂⁺

Only crude upper limits can be inferred for these heats of formation, but we include them for completeness. Thus,

TABLE II. Heats of formation for Si₂H_n⁺ species (kcal/mol at 0 K). Values in parentheses in present results are possible lower values. Values without parentheses are rigorous upper limits.

	Present results ^a	Potzinger and Lampe ^b	Boo and Armen- trout ^c	Curtiss <i>et al.</i> ^d
Si ₂ H ₆ ⁺	247.5 ± 0.6	258	...	243.5
Si ₂ H ₅ ⁺	<238.5 ± 0.6 (234.4 ± 0.8)	235	...	232.5
Si ₂ H ₄ ⁺	254.4 ± 0.6[H ₂ SiSiH ₂ ⁺] <272.2 ± 0.6[H ₃ SiSiH ⁺]	274	...	253.5 267.1
Si ₂ H ₃ ⁺	<271.1 ± 0.9 (<264)	260	264.5 (2)	258.5
Si ₂ H ₂ ⁺	<293.1 ^{+0.6} _{-1.0} (<289.7 ± 0.8) (~283)	296	<265.5 (2.6)	284.2
Si ₂ H ⁺	<317	269	<302.9 (1.6)	306.4
Si ₂ ⁺	<357	(323) ^e	<326.5 (2)	322.7

^aBased on $\Delta H_f^0(\text{Si}_2\text{H}_6) = 22.9 \pm 0.3$ kcal/mol.

^bFrom Ref. 28. These authors used $\Delta H_{f, \text{gas}}^0(\text{Si}_2\text{H}_6) = 17.1$ kcal/mol. We have adjusted their values to the present convention, $\Delta H_f^0(\text{Si}_2\text{H}_6) = 22.9$ kcal/mol.

^cFrom Ref. 44. Their values are given for 298 K, using the thermal electron convention. We have corrected them to 0 K.

^dReference 22

^eNot given by Potzinger and Lampe, but calculated from their appearance potential.

$\Delta H_f^0(\text{Si}_2\text{H}^+) < 317$ kcal/mol, and $\Delta H_f^0(\text{Si}_2^+) < 357$ kcal/mol.

All of the above heats of formation are collected in Table II, and compared with other experimental and calculated values. The comparisons with the experimental values of Potzinger and Lampe²⁸ and the *ab initio* calculations of Curtiss *et al.*²² follow the same trends discussed for Table I. Also included in Table II are heats of formation (modified) based on ion-impact thresholds, primarily Si⁺ + SiH₄, obtained by Boo and Armentrout.⁴⁴ From the nature of their experiment, their values for $\Delta H_f^0(\text{Si}_2^+)$ and $\Delta H_f^0(\text{Si}_2\text{H}^+)$ are expected to be much better than the photoionization values. For $\Delta H_f^0(\text{Si}_2\text{H}_3^+)$ the two experimental values are comparable. However, for $\Delta H_f^0(\text{Si}_2\text{H}_2^+)$, the ion-impact value (based on the reaction of a different projectile, SiH⁺) are about 20 kcal/mol lower than photoionization and calculated values, and appear to be in error.

V. DISCUSSION

The photoionization experiments on Si₂H₆ reveal the presence of two quasilinear regions in the photoion yield curve, and hence two onsets for Si₂H₄⁺. We have attributed them to two differing configurations: (a) H₂SiSiH₂⁺, which appears first (and is therefore more stable), but which has difficulty in forming from Si₂H₆; and (b) H₃Si-SiH⁺, which is less stable, but forms more readily by 1,1-H₂ elimination. A direct proof of these attributions could be forthcoming if a sample of H₃Si-SiD₃ were available, and if scrambling did not occur, but (to our knowledge) such a selectively deuterated disilane has not yet been prepared.

The presence of two onsets, as well as the values of the appearance potentials themselves, find support in *ab initio* calculations.²² However, additional *ab initio* calculations³⁹ predict a reverse activation barrier of 20 kcal/mol for the lower-energy process. If our interpretation of this lower energy process is correct, it is not at all clear why we are able to observe it.

VI. CONCLUSIONS

Photoionization mass spectrometric studies of Si₂H₆ yield the following results (in eV at 0 K): I.P. (Si₂H₆) = 9.74 ± 0.02; A.P. (Si₂H₅⁺) < 11.59 ± 0.02 (11.41 ± 0.03); A.P. (Si₂H₄⁺, sym) < 10.04 ± 0.02; A.P. (Si₂H₄⁺, asym) < 10.81 ± 0.02; A.P. (Si₂H₃⁺) < 13.00 ± 0.04 (< 12.70); A.P. (Si₂H₂⁺) < 11.72^{+0.02}_{-0.04} (< 11.57 ± 0.03); and A.P. (SiH₃⁺) < 11.72 ± 0.02. The appearance potentials of Si₂H⁺ and Si₂⁺ obtained are crude upper limits. The experimental values for Si₂H₆⁺, Si₂H₅⁺, and Si₂H₄⁺ are in good agreement with *ab initio* calculations. For the other species, the experimental values are higher than the calculated ones, as expected.

ACKNOWLEDGMENT

This research was supported by the U.S. Department of Energy (Office of Basic Energy Sciences) under Contract No. W-31-109-Eng-38.

¹M. L. Mandich, W. D. Reents, Jr., and K. D. Kolenbrander, *J. Chem. Phys.* **92**, 437 (1990); M. L. Mandich, W. D. Reents, Jr., and M. F. Jarrold, *ibid.* **88**, 1703 (1988).

- ²J. Berkowitz, J. P. Greene, H. Cho, and B. Ruscic, *J. Chem. Phys.* **86**, 1235 (1987).
- ³L. A. Curtiss and J. A. Pople, *Chem. Phys. Lett.* **144**, 38 (1988).
- ⁴H.-J. Kohler and H. Lischka, *Chem. Phys. Lett.* **112**, 33 (1984).
- ⁵H.-J. Kohler and H. Lischka, *Chem. Phys. Lett.* **98**, 454 (1983).
- ⁶H. Lischka and H.-J. Kohler, *J. Am. Chem. Soc.* **105**, 6646 (1983).
- ⁷H. Lischka and H.-J. Kohler, *Chem. Phys. Lett.* **85**, 467 (1982).
- ⁸H. J. Kohler and H. Lischka, *J. Am. Chem. Soc.* **104**, 5884 (1982).
- ⁹P. Ho and C. F. Melius, *J. Phys. Chem.* **94**, 5120 (1990).
- ¹⁰P. Ho, M. E. Coltrin, J. S. Binkley, and C. F. Melius, *J. Phys. Chem.* **90**, 3399 (1986).
- ¹¹J. S. Binkley, *J. Am. Chem. Soc.* **106**, 603 (1984).
- ¹²D. S. Horowitz and W. A. Goddard III, *J. Mol. Struct.* **163**, 207 (1988).
- ¹³J. A. Boatz and M. S. Gordon, *J. Phys. Chem.* **94**, 7331 (1990).
- ¹⁴M. S. Gordon, T. N. Truong, and E. K. Bonderson, *J. Am. Chem. Soc.* **108**, 421 (1986).
- ¹⁵B. T. Colegrove and H. F. Schaefer III, *J. Chem. Phys.* **93**, 7230 (1990).
- ¹⁶B. T. Colegrove and H. F. Schaefer III, *J. Phys. Chem.* **94**, 5593 (1990).
- ¹⁷A. F. Sax and J. Kalcher, *J. Phys. Chem.* **95**, 1768 (1991).
- ¹⁸J. Kalcher, A. Sax, and G. Olbrich, *Int. J. Quantum Chem.* **25**, 543 (1984).
- ¹⁹G. Olbrich, *Chem. Phys. Lett.* **130**, 115 (1986).
- ²⁰K. Raghavachari, *J. Chem. Phys.* **92**, 452 (1990).
- ²¹K. Raghavachari, *J. Chem. Phys.* **88**, 1688 (1988).
- ²²L. A. Curtiss, K. Raghavachari, P. W. Deutsch, and J. A. Pople, *J. Chem. Phys.* (submitted).
- ²³R. S. Grev, B. J. Deleeuw, and H. F. Schaefer III, *Chem. Phys. Lett.* **165**, 257 (1990).
- ²⁴B. Ruscic and J. Berkowitz, *J. Chem. Phys.* **95**, 2416 (1991).
- ²⁵S. T. Gibson, J. P. Greene, and J. Berkowitz, *J. Chem. Phys.* **83**, 4319 (1985).
- ²⁶H. Bock, *Angew. Chem. Int. Ed.* **28**, 1627 (1989); see also H. Bock, W. Ensslin, F. Feher, and R. Freund, *J. Am. Chem. Soc.* **98**, 668 (1976).
- ²⁷P. De Bievre, M. Gallet, N. E. Holden, and I. L. Barnes, *J. Phys. Chem. Ref. Data* **13**, 809 (1984).
- ²⁸P. Potzinger and F. W. Lampe, *J. Phys. Chem.* **73**, 3912 (1969).
- ²⁹K. Watanabe, *J. Chem. Phys.* **26**, 542 (1957); **22**, 1564 (1954).
- ³⁰H. Chatham, D. Hils, R. Robertson, and A. Gallagher, *J. Chem. Phys.* **81**, 1770 (1984).
- ³¹P. Potzinger, A. Ritter, and J. Krause, *Z. Naturforsch.* **30a**, 347 (1975).
- ³²S. G. Lias, J. E. Bartmess, J. F. Liebman, J. L. Holmes, R. D. Levin, and G. W. Mallard, *J. Phys. Chem. Ref. Data* **17**, Suppl. 1, 623 (1988).
- ³³The rationale for making this correction is given by P. M. Guyon and J. Berkowitz, *J. Chem. Phys.* **54**, 1814 (1971). The actual computation for Si₂H₆ is given in Ref. 25.
- ³⁴See, for example, J. Berkowitz, *Photoabsorption, Photoionization and Photoelectron Spectroscopy* (Academic, New York, 1979), p. 305.
- ³⁵J. Berkowitz, Ref. 34, pp. 300–301.
- ³⁶H. M. Rosenstock, R. Buff, M. A. A. Ferreria, S. G. Lias, A. C. Parr, R. L. Stockbauer, and J. L. Holmes, *J. Am. Chem. Soc.* **104**, 2337 (1982).
- ³⁷Landolt-Bornstein Tables, New Series, Vol. 7, *Structure Data of Free Polyatomic Molecules* (Springer-Verlag, Berlin, 1976), p. 95.
- ³⁸G. W. Bethke and M. K. Wilson, *J. Chem. Phys.* **26**, 1107 (1957); J. R. Durig and J. S. Church, *J. Chem. Phys.* **73**, 4784 (1980).
- ³⁹K. Raghavachari (private communication).
- ⁴⁰R. E. Kutina, G. L. Goodman, and J. Berkowitz, *J. Chem. Phys.* **77**, 1664 (1982).
- ⁴¹Z. Prasil and W. Forst, *J. Phys. Chem.* **71**, 3166 (1967).
- ⁴²S. R. Gunn and L. G. Green, *J. Phys. Chem.* **65**, 779 (1961).
- ⁴³M. W. Chase, Jr., C. A. Davies, J. R. Downey, Jr., D. J. Frurip, R. A. McDonald, and A. N. Syverud, *J. Phys. Chem. Ref. Data* **14**, Suppl. 1, 1211 (1985).
- ⁴⁴B. H. Boo and P. B. Armentrout, *J. Am. Chem. Soc.* **109**, 3549 (1987).